

The Mass Assembly History of Galaxies and Clusters of Galaxies

Tadayuki Kodama¹, the PISCES team and the SXDS team

¹National Astronomical Observatory of Japan, Mitaka, Tokyo 181-8588, Japan
email: kodama@th.nao.ac.jp

Abstract.

We discuss the mass assembly history both on cluster and galaxy scales and their impact on galaxy evolution.

On cluster scale, we introduce our on-going PISCES project on Subaru, which plans to target ~ 15 clusters at $0.4 \leq z \leq 1.3$ using the unique wide-field ($30'$) optical camera Suprime-Cam and the spectrograph both in optical (FOCAS, $6'$) and near-infrared (FMOS, $30'$). The main objectives of this project are twofold: (1) Mapping out the large scale structures in and around the clusters on $10\text{--}14$ Mpc scale to study the hierarchical growth of clusters through assembly of surrounding groups. (2) Investigating the environmental variation of galaxy properties along the structures to study the origin of the morphology-density and star formation-density relations. Some initial results are presented.

On galactic scale, we first present the stellar mass growth of cluster galaxies out to $z \sim 1.5$ based on the near-infrared imaging of distant clusters and show that the mass assembly process of galaxies is largely completed by $z \sim 1.5$ and is faster than the current semi-analytic models' predictions. We then focus on the faint end of the luminosity function at $z \sim 1$ based on the Subaru/XMM-Newton Deep Survey imaging data. We show the deficit of red galaxies below $M^* + 2$ or $10^{10} M_\odot$, which suggest less massive galaxies are either genuinely young or still vigorously forming stars in sharp contrast to the massive galaxies where mass is assembled and star formation is terminated long time ago.

1. Panoramic Imaging and Spectroscopy of Cluster Evolution with Subaru (PISCES)

PISCES is a panoramic imaging survey of distant clusters using the Subaru wide-field optical camera Suprime-Cam which provides $34' \times 27'$ field of view corresponding to a physical area of 16×13 Mpc² at $z \sim 1$. This long term project has started since 2003, and we aim to target ~ 15 X-ray selected distant clusters in total at $0.4 \leq z \leq 1.3$, in good coordination with *ACS/HST*, *XMM*, and *Chandra* observations. This unique project is currently underway and some preliminary results on the large scale structures over the entire Suprime-Cam fields are shown in Figs. 1 and 2. These two rich clusters at $z=0.55$ and 0.83 were imaged in multi optical bands, and photometric redshifts (Kodama *et al.* 1999) have been applied to efficiently remove foreground/background contaminations and isolate the cluster member candidates (c.f. Kodama *et al.* 2001). Many substructures are then clearly seen around the main body of the clusters which tend to be aligned in filamentary structures extending to >10 Mpc scale across. Although these structures should be confirmed spectroscopically later on, these already provide good evidence for cluster scale assembly in the hierarchical Universe.

The large scale structures that we see around the clusters provide us the unique opportunities to look into the environmental effects on galaxies as they assemble to denser regions. Kodama *et al.* (2001) have presented the environmental dependence of

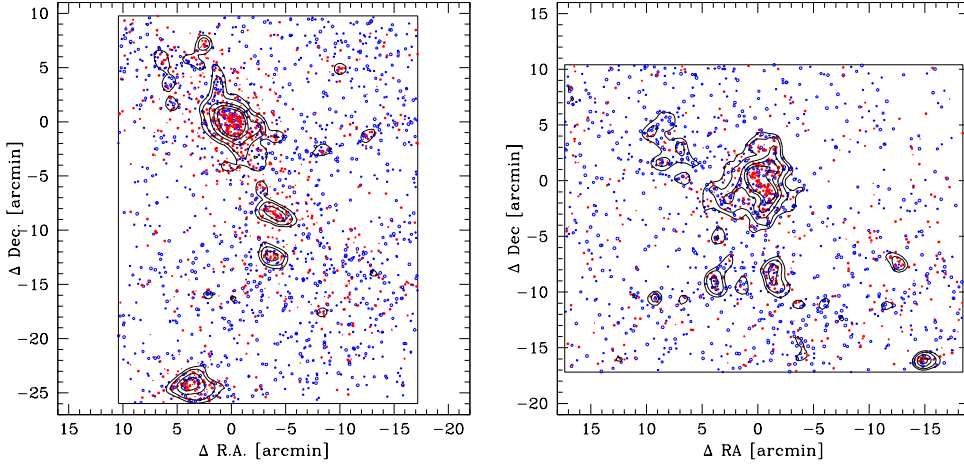


Figure 1. The panoramic maps of CL0016+16 cluster ($z=0.55$; left panel) and RXJ0152.7–1357 ($z=0.83$; right panel). 10 arcminutes correspond to physical scales of 3.8 and 4.6 Mpc, respectively. Using photometric redshift technique based on multi-colour data ($BVRi'z'$ and $VRi'z'$, respectively), plotted are the photometric member candidates selected with redshift cuts of $0.50 \leq z \leq 0.58$ and $0.78 \leq z \leq 0.86$, respectively. Contours show local 2-D number density of galaxies at $1.5, 2, 3, 4, 5 \sigma$ above the mean density. Coordinates are shown relative to the centre of the main cluster. Large scale filamentary structures (>10 Mpc) are seen in both clusters.

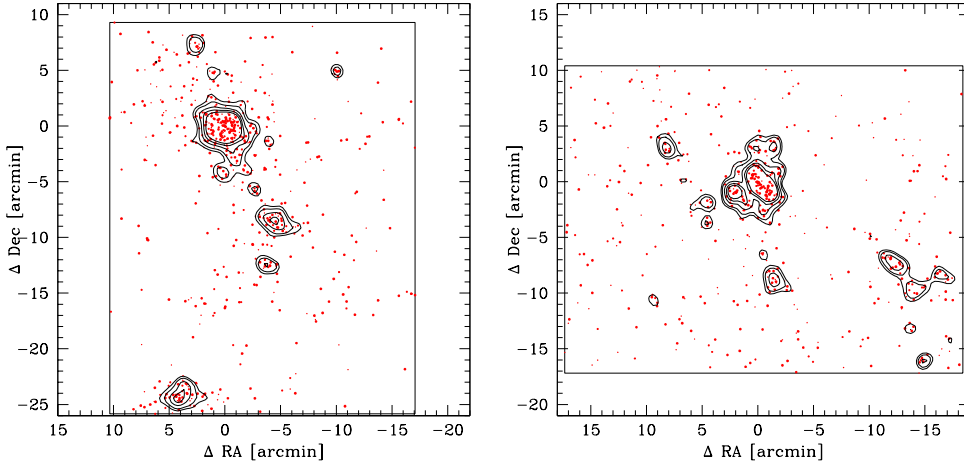


Figure 2. The same as Fig. 1, but only red galaxies on the colour-magnitude sequence are shown rather than phot- z selected galaxies. The red galaxies are selected on the basis of VRi' colours for CL0016+16 and $Ri'z'$ colours for RXJ0152.7–1357, respectively, and some red colour slice cuts are applied to isolate the passively evolving galaxies at cluster redshifts. This technique gives narrower redshift slice ($\Delta z \sim 0.05$) hence has less projection effect, but tends to be biased to the systems dominated by red populations. It is therefore complementary to the phot- z slice technique used in Fig. 1.

galaxy colours along the filamentary structures around the CL0939+47 cluster at $z=0.41$. They have shown that the galaxy colours change rather sharply at relatively low density regions such as galaxy groups along the filaments well outside of the cluster core where the galaxies have not yet passed the central region of the clusters yet (see also

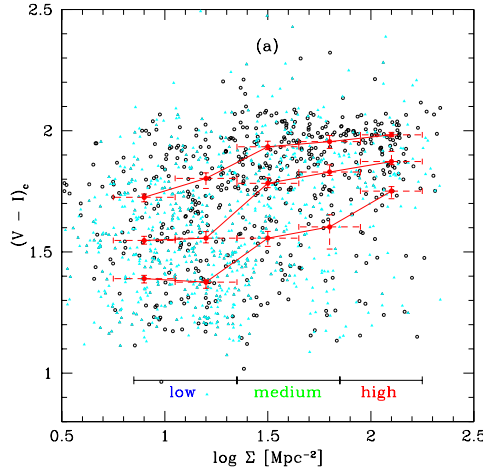


Figure 3. The variation in colour versus local galaxy density, for phot- z selected cluster members brighter than $I = 23.4$ in CL0939+47 cluster at $z = 0.41$ (Kodama *et al.* 2001). The open circles and filled triangles show the galaxies brighter or fainter than $I = 21.4$ ($M_V^* + 2$), respectively. The three red lines represent the loci of the 25, 50, and 75th percentile colours. The local number density is calculated from the 10 nearest galaxies and we correct this for residual field contamination in the photometric members using the blank field data.

Gray *et al.* 2004; Treu *et al.* 2003). Together with the similar findings in the local Universe (Lewis *et al.* 2002; Gomez *et al.* 2003), the environmental effects that truncate star formation are not driven by the cluster specific mechanism such as ram-pressure stripping (Abadi *et al.* 1999) and but are found to be much wider spread into low density regions. We should therefore pay greater attention to galaxy groups as the key hierarchy for the environmental effects and try to identify what is happening on galaxies in this environment (see below). It is also important to extend this analysis to higher redshifts as the galaxy environment should change dramatically during the course of vigorous assembly, which is probably related to the appearance of morphology-density relation (Dressler 1980).

Obviously, taking as many spectra as possible from the photometrically identified large scale structures is crucial to prove their reality, since our photometric approach may well suffer from the projection effect along the line of site as we go to lower density regions due to the broad phot- z slice cuts that we apply. Importantly, OII line and/or the 4000Å break feature are detectable for our PISCES targets in the optical spectroscopy (such as FOCAS) and H α line comes to the FMOS window ($0.9\mu\text{m} < \lambda < 1.8\mu\text{m}$). Not only definitively removing the foreground/background contamination and identifying the physically associated real groups, spectroscopic redshifts of individual cluster members will also provide us two critical information: (1) Dynamical mass of the systems which can then be compared to lensing mass and the X-ray mass to address the dynamical state of the systems. (2) 3-D velocity structures, providing the recent and/or near future cluster-cluster/cluster-group merger histories (e.g. Czoske *et al.* 2002).

Also, OII and H α lines will offer the measures of on-going star formation rate of galaxies. (The latter is preferred since it is much less affected by dust extinction or metallicity variation (Kennicutt *et al.* 1984)). Therefore we can directly identify when, where and on what timescale the star formation is truncated as the galaxies/groups fall into clusters along the filaments (e.g. Kodama *et al.* 2004b). Moreover, we will combine the information from other spectral indices such as Balmer lines and colours in order to

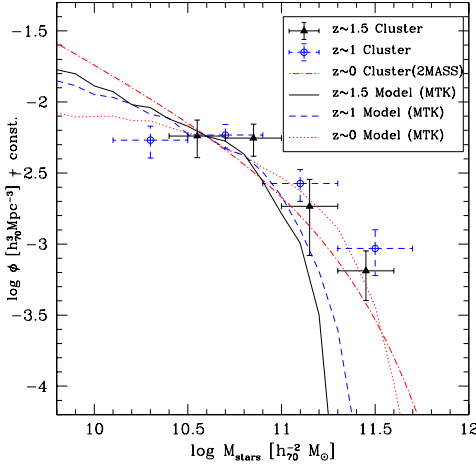


Figure 4. Stellar mass functions of galaxies in clusters as a function of redshift. The Kennicutt's initial mass function (Kennicutt 1983) is used to scale the stellar mass. The open diamonds and the filled triangles show the stellar mass functions for $z \sim 1$ and $z \sim 1.5$ clusters, respectively, which are compared to the local counterpart from the 2MASS survey (dot-dashed curve). All the curves and the data points are normalized at $5 \times 10^{10} M_\odot$ so as to have the same amplitude. The theoretical predictions from a semi-analytic model (Nagashima *et al.* 2002) are presented for comparison, which are made for galaxies in the haloes whose circular velocities are greater than 1000 km/s at each epoch. The mass assembly of massive galaxies in the real Universe is much faster than the hierarchical model prediction.

resolve the recent star formation histories in galaxies in fine time scales. Different spectral features are sensitive to different stellar ages (Kennicutt *et al.* 1984; Balogh *et al.* 1999; Poggianti *et al.* 1999): the emission lines (OII H α) will measure the amplitude of on-going star formation (10^7 yrs), while the Balmer absorption line give the luminosity (mass) contribution from the stars formed immediately before the truncation (10^{8-9} yrs) (Dressler & Gunn 1992; Couch & Sharples 1987) and the 4000Å break and broad-band colours specify the features of longer-lived populations ($>10^9$ yrs) (Kodama & Bower 2001). Resolving the recent star formation histories in galaxies in the transition regions (groups) is the key to understanding the physical processes behind the truncation. In particular, the existence of strong nebular emissions would support the galaxy-galaxy mergers which trigger star-burst, and very strong Balmer absorption line (E+A or k+a) would follow in the post star-burst phase (Poggianti *et al.* 1999). If the star formation is more gradually truncated ($\gtrsim 1$ Gyr) due to halo gas stripping (strangulation), we would not see any excess of E+A/k+a features (Balogh *et al.* 1999).

It is also important to investigate the morphologies of the galaxies in these groups. The key question here is whether the transformation of morphologies is driven by the same mechanisms as those responsible for the truncation of star formation (Poggianti *et al.* 1999; Treu *et al.* 2003). Furthermore, stellar mass function of galaxies (see §2) in groups compared to other environment will provide information on galaxy-galaxy merger in this hierarchy since the mergers increase the fraction of massive galaxies. On the contrary, strangulation does not change mass, hence can be distinguished by this test.

2. Stellar mass assembly of massive galaxies in high- z clusters

We now move on to the galactic scale, and firstly we present the stellar mass functions of galaxies in high- z clusters constructed from deep near-infrared imaging in J and K_s

(Fig. 4) (Kodama & Bower 2003a; Kodama *et al.* 2003b). The stellar mass function of galaxies derived from the K -band observations is a good tracer of mass assembly history of galaxies and therefore provides a critical test for the CDM-based bottom-up picture (e.g. Kauffmann & Charlot 1998; Baugh *et al.* 2002).

We have combined two $z \sim 1$ clusters (3C336 and Q1335+28; Kodama & Bower 2003a) and five $z \sim 1.5$ clusters (Q0835+580, Q1126+101, Q1258+404, Q0139-273, and Q2025-155; Hall *et al.* 1998; 2001; Best *et al.* 2003) to increase statistics. We have subtracted the control field counts taken from the literature (Saracco *et al.* 1999; Saracco *et al.* 2001; Best *et al.* 2003). Applying the same technique described in Kodama & Bower *et al.* (2003), we construct the field-subtracted stellar mass functions of galaxies in high- z clusters, primarily using K_s -band flux and also using $J - K_s$ colour as a measure of the M/L ratio. As shown, little evolution is observed since $z = 1.5$ to the present-day (2MASS clusters; Balogh *et al.* 2001), indicating that the mass assembly on galaxy scale is largely completed by $z \sim 1.5$ in the cluster environment. This epoch of mass assembly of massive galaxies is earlier than the prediction of the hierarchical models as shown for comparison (Nagashima *et al.* 2002).

It is interesting to apply similar analyses for the general field, since the high density regions may be the special places where galaxy formation processes take place in an accelerated way. Recently, Pozzetti *et al.* (2003) and Glazebrook *et al.* (2004) investigated the stellar mass growth of massive galaxies out to $z \sim 1.5$ based on the large (mostly) spectroscopic sample in $K20$ (52 arcmin^2) and $GDDS$ (120 arcmin^2), respectively, and found no or little evolution is seen in the stellar mass of massive galaxies, suggesting the early assembly of galaxies even in the general field environment.

It is also important to go even higher redshifts to firstly identify the epoch of assembly of massive galaxies when they start to break down into pieces. Recent deep NIR observations in fact start to enter such formation epoch (e.g. Dickinson *et al.* 2003; Franx *et al.* 2003; Rudnick *et al.* 2003; Daddi *et al.* 2003), and this aspect will be further extended by on-going and near future space missions such as *SIRTF* (Dickinson *et al.* 2002; Pozzetti *et al.*, 2003) and *Astro-F* (Japanese mission).

3. Down-sizing in galaxy formation seen at $z \sim 1$

It is known that the galaxy properties depend on mass or luminosity as well. Using the SDSS data, Kauffmann *et al.* (2003) and Baldry *et al.*, (2004) have shown an interesting break mass at $3 \times 10^{10} M_{\odot}$ above which the dominant population is red passively evolving galaxies, while below that mass the contribution of blue active galaxies become dominant. Morphological mix of galaxies is also known to be strongly luminosity (or stellar mass) dependent (e.g. Treu *et al.* 2003). It is therefore indicative that the formation of massive galaxies and less massive galaxies are quite different, in the sense that massive and/or early-type galaxies form early in the Universe, while dwarf and/or late-type galaxies form later on average or still forming stars at present. The mass dependent star formation history is referred to as “down-sizing” (Cowie *et al.* 1996).

Given the down-sizing effect in the local Universe, as we look back into higher redshift Universe, we expect to go beyond the formation epoch of small galaxies or towards the early stage of their formation, as well as to approach the formation epoch of more massive galaxies. To test this hypothesis, we investigate the galaxy colours at $z \sim 1$ as a function of luminosity (or stellar mass) utilizing the unique Suprime-Cam imaging data-set ($BRi'z'$) on the Subaru/XMM-Newton Deep Survey (SXDS). These data are both sufficiently deep ($z'_{AB}=25$, $6-10\sigma$) and wide (1.2 deg^2), which enable us for the first time to investigate the photometric properties of statistical sample of galaxies at

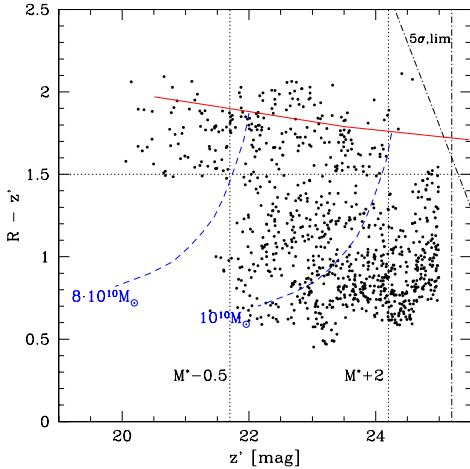


Figure 5. Field-corrected colour-magnitude diagram for the $z \sim 1$ galaxies in high density regions in SXDS (Kodama *et al.* 2004a). The solid line shows the expected location of colour-magnitude sequence at $z \sim 1$ assuming a passive evolution with $z_{\text{form}}=5$ (Kodama *et al.* 1998). The deficit of both blue galaxies at the bright/massive end and the deficit of red galaxies at the faint/less-massive end are both clearly identified. The stellar masses are scaled using the Kennicutt's IMF (Kennicutt 1983).

$z \sim 1$ down to $\sim M^*+3$ with respect to the passive evolution. We first identify five $z \sim 1$ high density regions by applying colour cuts at $1.7 < R - z' < 2.0$ and $0.8 < i' - z' < 1.1$, which correspond to the colours of passively evolving galaxies at $z \sim 1$ (Kodama *et al.* 1998). We then combine these five regions (amounting to 141 arcmin^2 in total) and subtract off the low density regions at $z \sim 1$ sampled from the same data-set and scaled to the same area. We do this subtraction on the colour-magnitude diagram (Kodama & Bower 2001) and isolate the $z \sim 1$ galaxies in a statistical sense. This method should work since both high and low density regions at $z \sim 1$ are expected to have the same amount of foreground/background contaminations.

The field-corrected colour-magnitude diagram thus constructed for $z \sim 1$ galaxies in high density regions is shown in Fig. 5. The most striking feature in the galaxy distribution on this diagram is that the galaxies are separated into two distinct populations, ‘bright+red’ and ‘faint+blue’. More precisely, we show a deficit of red and faint galaxies below M^*+2 or $10^{10} M_\odot$ in stellar mass and a lack of blue massive galaxies above $M^*-0.5$ or $8 \times 10^{10} M_\odot$ in stellar mass. The down-sizing in star formation is therefore also seen at high redshift, where star formation in massive galaxies takes place early in the Universe and is already truncated by $z \sim 1$, while almost all of small galaxies are still forming stars at $z \sim 1$ (Kodama *et al.* 2004a; Poggianti *et al.* 2004; see also De Lucia *et al.* in this volume). Together with the early-assembly of massive galaxies seen in § 2, galaxy formation does in fact take place in “down-sizing” fashion as apparently opposed to the “bottom-up” scenario. Some critical physical mechanisms in galaxy formation may be still missing in the current models.

It is important to note that there are two possible interpretations for the blue colours of faint galaxies. One is that they are just forming, and the other is that they have much extended star formation over the long period of time. To separate out these two possibilities, the key quantity to measure is the so-called birth-rate parameter (b) of these faint blue galaxies (Kennicutt 1988). Here b' is re-defined as on-going star formation rate

divided by integrated stellar mass of the system ($b' = SFR/M_{\text{stars}}$). SFR can be derived from OII and H α line intensities by spectroscopy or narrow-band imaging of the PISCES clusters and the SXDS field while M_{stars} can be obtained from the deep NIR imaging. This parameter describes what phase of star formation each galaxy is in, and therefore can discriminate between genuinely young galaxies formed recently (large b') and star forming galaxies formed long time ago (small b'). It is also interesting to directly detect the brightening of the break luminosity or mass with increasing redshift by going even higher redshifts.

References

Abadi, M. G., Moore, B., Bower, R. G., 1999, MNRAS, 308, 947
 Baldry I. K., *et al.*, 2004, ApJ, 600, 681
 Balogh M. L., *et al.*, 1999, ApJ, 527, 54
 Balogh, M. L., Christlein, D., Zabludoff, A. I., Zaritsky, D., 2001, ApJ, 557, 117
 Baugh, C. M., Benson, A. J., Cole, S., Frenk, C. S., Lacey, C., 2002, astro-ph/0203051
 Best, P. N., Lehnert, M. D., Miley, G. K., Röttgering, H. J. A., 2003, MNRAS, 343, 1
 Butcher, H., Oemler, A., 1984, ApJ, 285, 426
 Couch, W. J., Sharples, R. M., 1987, MNRAS, 229, 423
 Cowie, L. L., Songaila, A., Hu, E. M., Cohen, J. G., 1996, AJ, 112, 839
 Czoske, O., *et al.*, 2002, A&A, 386, 31
 Daddi, E., *et al.*, 2003, astro-ph/0308456
 Dickinson, M., Giavalisco, M., *et al.*, astro-ph/0204213
 Dickinson, M., Papovich, C., Ferguson, H. C., Budavari, T., 2003, ApJ, 587, 25
 Dressler, A., 1980, ApJ, 236, 351
 Dressler, A., Gunn, J. E., 1992, ApJS, 78, 1
 Finn, R. A., Zaritsky, D., McCarthey, D. W., 2004, ApJ, 604, 141
 Franx, M., *et al.*, 2003, ApJ, 587, L79
 Glazebrook, K., *et al.*, 2004, astro-ph/0401037
 Gómez, P. L., *et al.*, 2003, ApJ, 584, 210
 Gray M. E., *et al.*, 2004, MNRAS, 347, L73
 Kauffmann, G., Charlot, C., 1998, MNRAS, 297, 23
 Kauffmann, G., *et al.*, 2003, MNRAS, 341, 54
 Kennicutt, R. C., 1983, ApJ, 272, 54
 Kennicutt, R. C., *et al.*, 1994, ApJ, 435, 22
 Kennicutt, R. C., 1988, ARA&A, 36, 189
 Kodama, T., Arimoto, N., Barger, A. J., Aragón-Salamanca, A., 1998, A&A, 334, 99
 Kodama, T., Bell, E. F., Bower, R. G., 1999, MNRAS, 302, 152
 Kodama, T., Smail, I., Nakata, F., Okamura, S., Bower, R. G., 2001, ApJ, 562, L9
 Kodama, T., Bower, R. G., 2001, MNRAS, 321, 18
 Kodama, T., Bower, R. G., 2003a, MNRAS, 346, 1
 Kodama, T., *et al.* 2003b, astro-ph/0312321
 Kodama, T., *et al.*, 2004a, MNRAS, in press
 Kodama, T., Balogh, M. L., *et al.*, 2004b, in prep.
 Hall, P. B., Green, R. F., Cohen, M., 1998, ApJS, 119, 1
 Hall, P. B., *et al.*, 2001, AJ, 121, 1840
 Lewis, I., *et al.*, 2002, MNRAS, 334, 673
 Nagashima, M., Yoshii, Y., Totani, T., Gouda, N., 2002, ApJ, 578, 675
 Poggianti, B. M. *et al.* 1999, ApJ, 518, 576
 Poggianti, B. M. *et al.* 2004, ApJ, 601, 197
 Pozzetti, L., *et al.*, 2003, A&A, 402, 837
 Rudnick, G., *et al.*, 2003, astro-ph/0307149
 Saracco, P., *et al.*, 1999, A&A, 349, 751
 Saracco, P., *et al.*, 2001, A&A, 375, 1

